PO Box 2345, Beijing 100023, China
www.wjgnet.com
wjg@wjgnet.com

ELSEVIER

World J Gastroenterol 2005;11(28):4382-4389
World Journal of Gastroenterology ISSN 1007-9327

• *CLINICAL RESEARCH* •

Expression of adhesion molecules on mature cholangiocytes in canal of Hering and bile ductules in wedge biopsy samples of primary biliary cirrhosis

Hiroaki Yokomori, Masaya Oda, Mariko Ogi, Go Wakabayashi, Shigeyuki Kawachi, Kazunori Yoshimura, Toshihiro Nagai, Masaki Kitajima, Masahiko Nomura, Toshifumi Hibi

Hiroaki Yokomori, Department of Internal Medicine, Kitasato Institute Medical Center Hospital, Saitama 364-8501, Japan
Masaya Oda, Organized Center of Clinical Medicine, International University of Health and Welfare, Tokyo 107-0052, Japan
Mariko Ogi, Laboratory of Pathology, Kitasato Institute Medical Center Hospital, Saitama 364-8501, Japan
Go Wakabayashi, Shigeyuki Kawachi, Masaki Kitajima, Department of Surgery, School of Medicine, Keio University, Tokyo 160-0016, Japan
Kazunori Yoshimura, Masahiko Nomura, Physiology, Saitama Medical School, Saitama 350-0495, Japan
Toshihiro Nagai, Electron Microscopy Laboratory, School of Medicine, Keio University, Tokyo 160-0016, Japan
Toshifumi Hibi, Department of Internal Medicine, School of Medicine, Keio University, Tokyo 160-0016, Japan
Correspondence to: Hiroaki Yokomori, MD, Kitasato Institute Medical Center Hospital, 121-1 Arai, Kitamotoshi, Saitama 364-8501, Japan. yokomori-hr@kitasato.or.jp
Telephone: +81-485-93-1212 Fax: +81-485-93-1239
Received: 2004-07-28 Accepted: 2004-08-31

Abstract

AIM: To examine the expression of intercellular adhesion molecule-1 (ICAM-1) and lymphocyte function-associated antigen-1 (LFA-1) expression on canals of Hering (CoH) and bile ductules associated with the autoimmune process of bile duct destruction in primary biliary cirrhosis (PBC).

METHODS: Ten wedged liver biopsies of PBC (five cases each of stages 2 and 3) were studied. The liver specimens were processed for transmission electron microscopy. Immunohistochemistry was performed using anti-ICAM-1 and anti-LFA-1 mouse mAbs. *In situ* hybridization was done to examine the messenger RNA expression of ICAM-1 in formalin-fixed, paraffin-embedded sections using peptide nucleic acid probes and the catalyzed signal amplification (CSA) technique. Immunogold-silver staining for electron microscopy was performed using anti-ICAM and anti-LFA-1 mouse mAbs. The immunogold particles on epithelial cells of bile ductules and cholangiocytes of CoH cells were counted and analyzed semi-quantitatively. Western blotting was performed to confirm ICAM-1 protein expression.

RESULTS: In liver tissues of PBC patients, immunohistochemistry showed aberrant ICAM-1 expression on the plasma membrane of epithelial cells lining bile ductules, and also on mature cholangiocytes but not on hepatocytes in CoH. LFA-1-positive lymphocytes were closely associated with epithelial cells in bile ductules. ICAM-1 expression at protein level was confirmed by Western blot. *In situ* hybridization demonstrated ICAM-1 mRNA expression in bile ductules and LFA-1 mRNA in lymphocytes infiltrating the bile ductules. By immunoelectron microscopy, ICAM-1 was demonstrated on the basal surface of epithelial cells in bile ductules and on the luminal surfaces of cholangiocytes in damaged CoH. Cells with intermediate morphology resembling progenitor cells in CoH were not labeled with ICAM-1 and LFA-1.

CONCLUSION: *De novo* expression of ICAM-1 both on mature cholangiocytes in CoH and epithelial cells in bile ductules in PBC implies that lymphocyte-induced destruction through adhesion by ICAM-1 and binding of LFA-1-expressing activated lymphocytes takes place not only in bile ductules but also in the CoH.

Key words: Primary biliary cirrhosis; Canal of Hering; Small bile ductile; ICAM-1; LFA-1; Immunohistochemistry; Western blot; Immunogold electron microscopy

Yokomori H, Oda M, Ogi M, Wakabayashi G, Kawachi S, Yoshimura K, Nagai T, Kitajima M, Nomura M, Hibi T. Expression of adhesion molecules on mature cholangiocytes in canal of Hering and bile ductules in wedge biopsy samples of primary biliary cirrhosis. *World J Gastroenterol* 2005; 11(28): 4382-4389
http://www.wjgnet.com/1007-9327/11/4382.asp

INTRODUCTION

The canal of Hering (CoH) is named after Hering who in 1855 described the structure as a link between the hepatocyte canalicular system and biliary tree[1]. Under the electron microscope, the small cells of CoH have a basement membrane like the more distal portions of the biliary tree but an apical surface that appears similar to hepatic canalicular membrane[2]. Functionally, bile canalicular contraction is involved in the canalicular bile flow as demonstrated by an inverted microscope linked to a SIT camera, and disturbance of canalicular contraction would lead to intrahepatic cholestasis[3]. Moreover, contraction of the CoH has been demonstrated, and the interval between contractions was approximately five times longer than that seen in canaliculi[4]. Hepatic cholestasis and hepatic injury are accompanied with

striking morphologic changes. Examination of periportal changes in the liver of graft-*vs*-host disease mice shows that hepatocytes in close contact with lymphocytes had minor degenerative changes, whereas periportal bile ductules and CoH are constantly injured by inflammatory cells[5]. Study of the three-dimensional structure of ductular reactions in massive necrosis suggests that cytokeratin 19-positive reactions are in fact proliferations of the cells lining the CoH[6].

Primary biliary cirrhosis (PBC) is a chronic, progressive cholestatic liver disease characterized by inflammatory obliteration of the intrahepatic bile ducts, leading to fibrosis and ultimately to cirrhosis complicated by liver failure or hypertention[7,8]. Although the pathogenesis of bile duct destruction in PBC remains unknown, increasing evidence has suggested that it is related to autoimmune abnormalities[8-10]. Immunohistochemical analysis of the lymphocytes infiltrating the portal tracts including the bile duct lesions indicates that activated T lymphocyte subsets may play an important role in bile duct destruction[11]. Therefore bile ducts (centrally located, accompanied by a hepatic arterial branch) are the prime targets for immune-mediated damages in PBC and are reduced in number as the disease progresses. Bile ductules (peripherally located, usually without a conspicuous lumen) increase in number in response to bile duct damage (ductular reaction). Bile ductules are frequently associated with a mixed population of inflammatory cells. However, there is no clear evidence that these inflammatory cells are associated with bile ductular destruction[12]. Recent studies have demonstrated increased expression of intercellular adhesion molecule (ICAM)-1 on the bile duct epithelium in PBC[13,14], suggesting that the activated T lymphocytes may specifically react with the bile duct epithelial cells through these adhesion molecules. Expression of intracellular adhesion molecules and their specific ligands are essential for cell-to-cell interactions in autoimmune mechanism[15]. In PBC, ICAM-1 is expressed on plasma membrane of epithelial cell in bile ducts characterized by chronic non-suppurative destructive cholangitis (CNSDC) and on the sinusoidal endothelial cells[16,17]. While immunohistochemical findings of ICAM-1 and lymphocyte function-associated antigen (LFA)-1 expression in PBC tissue have been reported[17], no studies have correlated protein expression of the antigens on CoH by examining serial sections using immunoelectron microscopy. The aim of the present study was to clarify the roles of ICAM-1 and LFA-1 expression on the bile ductule and CoH in PBC. The aim of the present study was to clarify ICAM-1 and LFA-1 expression on the bile ductule and CoH in PBC. We conducted immunohistochemistry, *in situ* hybridization and immunoelectron microscopy on liver biopsy specimens from PBC patients.

MATERIALS AND METHODS

Materials

Surgical liver biopsy specimens were obtained from 10 patients (all female, mean age 55.9 years, range 48-65 years) with PBC (five cases each of Scheuer's stages 2 and 3). PBC was diagnosed clinically and histologically according to the criteria proposed by the Japanese Joint Research Group for Autoi-mmune Hepatitis[18]. As controls, wedge biopsy specimens from normal portions of the liver were obtained from five patients (four male and one female; aged from 54 to 71 years with a mean of 62.6 years) who underwent surgical resection for metastatic liver carcinoma (four colonic carcinomas).

Electron microscopy

The liver specimens were cut into small blocks (approximately 1 mm×1 mm×1 mm). The blocks were fixed in fresh 2.5% glutaraldehyde solution for 1 h at 4 ℃, followed by post-fixation in 2% osmium tetroxide with 0.1 mol/L cacodylate buffer (pH 7.4), and then dehydrated in a graded series of ethanol solutions. For transmission electron microscopy, the liver tissue blocks were embedded in Epon after dehydration. Ultrathin sections were cut with a diamond knife on a LKB ultramicrotome (Bromma), stained with uranyl acetate and lead citrate and observed under a transmission electron microscope (JEM-1200 EX, JEOL, Tokyo, Japan) with a 80-kV acceleration voltage.

Immunohistochemical staining

Liver tissues (approximately 5 mm×5 mm×5 mm) were fixed in periodate-lysine-parafomaldehyde[19], rinsed in 0.01 mol/L phosphate buffer (pH 7.4) containing 15-30% sucrose, embedded in Tissue-Tek OCT-compound (Miles Inc., Elkhart. Inc., Germany) and frozen at -80 ℃ until use. The tissue was incubated overnight at 4 ℃ with anti-ICAM-1 mouse mAb (CD54; DAKO, Glostrup, Denmark) diluted at 1∶50 or anti-LFA-1 mouse mAb (CD11a; DAKO, Glostrup, Denmark) diluted at 1∶20, and then incubated with horseradish peroxidase-conjugated anti-mouse IgG goat antibody (Cosmo Bio Inc., Tokyo, Japan) diluted 1∶100. After repeated washes with PBS, the sections were reacted with diaminobenzidine solution containing 0.01% H_2O_2, and counterstained with hematoxylin for light-microscopic study.

In situ hybridization technique

Messenger RNA of ICAM-1 was detected in formalin-fixed, paraffin-embedded sections by *in situ* hybridization using peptide nucleic acid (PNA) probes[20] and the catalyzed signal amplification (CSA) technique. Liver tissues were cut into 4 μm-thick sections and adhered to silanated RNAse-free glass slides (prepared by heating in an oven at 60 ℃ for 30 min). The sections were dewaxed in xylene (for 15 min, each twice), treated with a graded ethanol series, rehydrated in RNAse-free distilled water, and incubated for 30 min in target retrieval buffer (DAKO Japan, Kyoto, Japan) preheated and maintained at 95 ℃. The slides were allowed to cool at room temperature for 20 min and then digested with 20 μg/mL proteinase K (DAKO) at room temperature for 30 min. The slides were rinsed in distilled water and rapidly air dried. The air-dried sections were covered with approximately 15 mL of hybridization solution containing 100 g/L dextran sulfate, 10 mmol/L NaCl, 300 mL/L formamide, 1 g/L sodium pyrophosphate, 2 g/L polyvinylpyrrolidone, 2 g/L Ficoll, 5 mmol/L Na_2EDTA, 50 mmol/L Tris-HCl, pH 7.5, and 1 μg/mL PNA probe. Probes were constructed according to the sequence information of ICAM-1 and LFA-1[21,22]. The following probes were used: ICAM-1 antisense (FITC-ATTATGACTGCGGCTGC), ICAM-1 sense (FITC-GCAGCCGCAGTCATAAT),

LFA-1 antisense (FITC-CATCCAGCTGCAGAGTGT), and LFA-1 sense (FITC-ACACTCTGCAGCTGGATG). The slides were evenly covered with the hybridization solution and incubated in a moist chamber at 43 ℃ for 90 min. Following hybridization, the cover slips were removed, and the slides were transferred to pre-warmed TBS in a water bath at 49 ℃ and washed for 30 min with gentle shaking (PNA Hybridization Kit; DAKO, Tokyo, Japan). A non-isotopic, colorimetric signal amplification system (GenPoint kit, DAKO Japan) was used to visualize specific hybridization signals. Briefly, tissue sections were incubated with a FITC–horseradish peroxidase reagent for 15 min, washed thrice with TBST (150 mmol/L NaCl, 10 mmol/L Tris; pH 7.5, 11 mL/L Tween 20), incubated with a solution containing H_2O_2 and biotinyl tyramide for 15 min, and washed thrice with TBST[23]. This step resulted in CSA by additional deposition of biotin at the site of probe hybridization. The sections were then incubated in streptavidin-horseradish peroxidase for 15 min, and washed thrice in TBST. Colorimetric signals were developed by incubation in diaminobenzidine solution containing 0.01% H_2O_2, and counterstained with hematoxylin for light microscopic examination.

Immunogold-silver staining method for electron microscopy

For light microscopy, the sections were immersed in three changes of 0.01% PBS (pH 7.4) for 15 min, and then incubated overnight in a moist chamber at 4 ℃ with anti-ICAM-1 mouse mAb at 1:50 dilution and anti-LFA-1 mouse mAb at 1:20 dilution. After washing thrice with PBS for 15 min, the sections were incubated for 40 min with 10-nm colloidal gold-conjugated anti-mouse IgG antibody (Cosmo Bio Co., Tokyo, Japan) diluted at 1:100. The slides were developed with a developing solution described below for 50 min at 20 ℃ in a dark room. After having washed in running water, the sections were briefly counterstained with 0.1% nuclear fast red in 5% aluminum sulfate aqueous solution, dehydrated, cleared and mounted on Biolet. The developing solution had two components. Solution A contained 45 mL of 20% gum arabic aqueous solution (Kanto Chemical Co., Tokyo, Japan) and 1 mL of 10% silver nitrate solution. The gum arabic solution was prepared by centrifuging a 20% suspension at 18 000 *g* for 30 min at 0 ℃ and separating the supernatant for use. Solution B contained 200 mg of hydroquinone (Kanto Chemical Co., Tokyo, Japan) and 300 mg of citric acid monohydrate (Kanto Chemical Co., Tokyo, Japan) in 10 mL of distilled water. The working developing solution was prepared by mixing solutions A and B in a dark room under illumination of a photographic safety lamp[24].

For electron microscopy, the tissue specimens processed for light microscopy as above were treated thrice, with PBS for 15 min, and fixed for 1 h at 4 ℃ in 1.2% glutaraldehyde buffered with 0.01% phosphate buffer (pH 7.4), followed by a graded series of ethanol solutions. After postfixation with 1% osmium tetroxide in 0.01% phosphate buffer (pH 7.4), the liver tissues were embedded in Epon. Ultrathin sections cut with a diamond knife on a LKB ultramicrotome were stained with uranyl acetate and observed under a transmission electron microscope (JEM-1200 EX, Tokyo, Japan) operated at an acceleration voltage of 80 kV.

Western blotting

Western blotting was conducted using fresh control and PBC liver tissues. Briefly, liver tissues were homogenized in 10 volumes of homogenization buffer (20 mmol/L Tris-HCl; pH 7.5, 5 mmol/L $MgCl_2$, 0.1 mmol/L PMSF, 20 μmol/L pepstatin A, and 20 μmol/L leupeptin) using a polytron homogenizer at setting 7 for 90 s. The homogenates were centrifuged at 100 000 *g* for 45 min. The membranes were washed thrice, resuspended in 10 volumes of homogenization buffer, homogenized using a Teflon/glass homogenizer, and centrifuged. The membrane proteins thus obtained were used for immunoblotting. Proteins were separated on SDS/PAGE (4-20% gel, Daiichi-Ikagaku, Tokyo, Japan) and transferred onto polyvinylidene difluoride (PVDF) membranes (Millipore, Bedford, MA). The blots were blocked with 50 g/L dried milk in PBS for 30 min, incubated with 20 μg/mL anti-ICAM-1 (G-5; Santa Cruz Bio., Santa Cruz, CA, USA), washed in 0.1% Tween 20 in PBS, and transferred onto PVDF membranes (NTN Life Science Products). The blots were blocked with 50 g/L dried milk in PBS for 30 min, incubated with anti-mouse goat IgG conjugated with horseradish peroxidase (Amershampharmacia) in 0.1% Tween 20 in PBS, and then processed by the Vectastain ABC system (Vector laboratories, Inc., Burlingame, CA, USA). The immunoreactive bands were visualized with diaminobenzidine solution containing 0.01% H_2O_2.

Semi-quantitative analysis

The immunogold particles on epithelial cells of bile ductules and cholangiocytes of CoH cells were counted. Photographs from 10 fields between the bile ductules and canal of Hering were investigated. The magnification was ×2 000.

RESULTS

Electron microscopic finding

Electron microscopic observation of the PBC liver specimens revealed lymphocytes associated with the bile ductular membrane in bile ductules (Figure 1A). Lymphocytes frequently migrated into the epithelial layer of CoH through their basement membrane (Figure 1B).

Immunohistochemical finding

We examined the immunohistochemical reactions of both ICAM-1 and LFA-1 in serial sections. In control liver specimens, ICAM-1 protein was expressed on sinusoidal lining cells but no specific immunoreactivity was observed on bile duct epithelial cells (Figure 2A). Immunostaining for LFA-1 appears to be present in portal lymphoid cells. Interlobular bile ducts appear to be negative for LFA-1, although there was sparse expression in bile duct epithelial cells (Figure 2B). In PBC liver tissue, *de novo* expression of ICAM-1 was found on the plasma membrane on the luminal side of epithelial cells in bile ductules and on some lymphocytes infiltrating small bile ductules or possibly small blood vessels. ICAM-1 immunoreactivity was also seen on the sinusoidal endothelial cells (Figure 2C). LFA-1 protein was expressed mainly in lymphocytes around and among the proliferated bile ductules (Figure 2D). Immunostaining of ICAM-1 and LFA-1 in CoH was less clearly depicted by immunostaining examined under a light microscope.

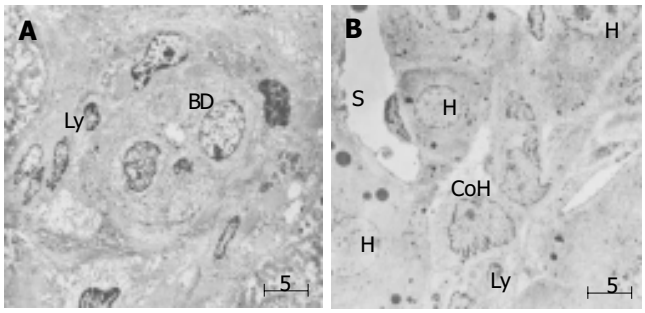

Figure 1 Electron microscopic finding in small bile ductule and CoH in liver specimen of PHC. **A:** Interaction of lymphocytes appear to interact with the bile ductule. Lymphocytes frequently migrate into the epithelial layer of small bile duct through the basement membrane. BD: bile ductule, ly: lymphocyte; **B:** Association of lymphocytes with the cholangiocytes of the CoH. CoH: canal of Hering. S: sinusoid, H: hepatocytes, Ly: lymphocytes, Bar: 5 μm.

Western blot

To confirm the immunohistochemical results, we investigated ICAM-1 protein expression by Western blotting. Samples containing 20 μg of protein were subjected to SDS/PAGE (4-20% gel) and analyzed by blotting with anti-ICAM-1 antibody. A band around 110 ku indicating ICAM-1 was found in abundance in PBC liver tissue (Figure 3).

In situ hybridization

Next, we investigated the expression of ICAM-1 and LFA-1 at mRNA level in PBC liver samples using *in situ* hybridization with PNA probes (Figure 4). Signals showing ICAM-1 mRNA were typically localized in bile ductular epithelial cells surrounding the CNSDC lesions (Figures 4A and B). Interestingly, signals showing LFA-1 were localized in lymphocytes inside the bile ductules of CNSDC lesions (Figures 4C and D).

Immuoelectron microscopy

Light microscopic examination of PBC liver samples depicted the localization of ICAM-1 and LFA-1 in bile ductules, but the localization in the CoH was less clear. We therefore conducted immunoelectron microscopic examin-ation. By immunogold electron microscopy, gold-labeled ICAM-1 particles were observed on cholangiocytes, distributing on the luminal surfaces of small bile ductules. ICAM-1 immunoreactivity was also observed on small portal or peripheral blood vessels and sinusoidal endothelial cells (Figure 5A). In the canal of Hering, gold-labeled ICAM-1 particles were observed on the luminal surfaces of cholangiocytes and hepatocytes (Figure 5C). LFA-1 labeling was concentrated on lymphocytes that were found around bile ductules (Figure 5B) and also around cholangiocytes of CoH (Figure 5D). Immature cells resembling progenitor cells were observed in CoH, and these cells did not show ICAM-1 immunoreactivity (Figure 5E). Around these cells, infiltration of lymphocytes was also absent (Figure 5F).

In the semi-quantitative analysis, immunogold–silver complex particles on epithelial cells of bile ductules and cholangiocytes of CoH were enumerated on immunoelectron micrographs (Figure 6). ICAM-1 immunoreactivity was found in CoH in 4 of the 10 PBC cases and in bile ductules

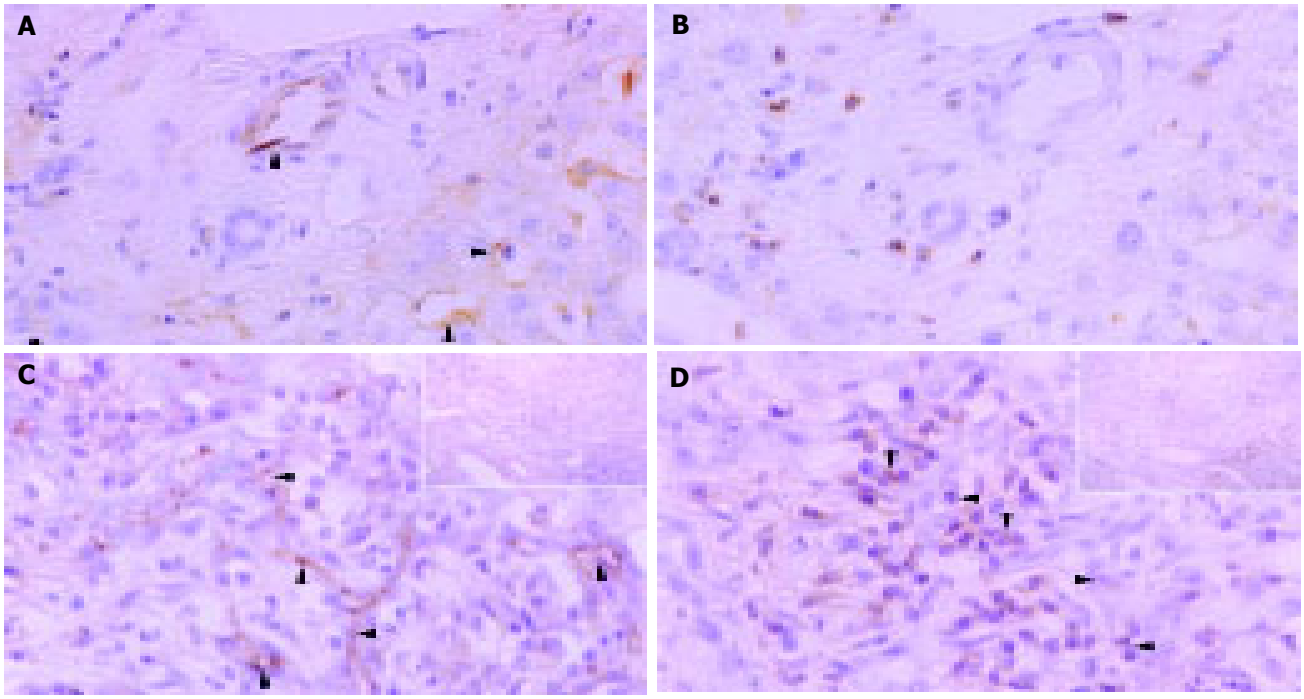

Figure 2 Immunohistochemical distributions of ICAM-1 (**A** and **C**) and LFA-1 (**B** and **D**) in control liver tissue (**A** and **D**) and liver tissue of PHC (**C** and **D**). **A:** ICAM-1 protein expression on sinusoidal lining cells but no specific immunoreactivity on bile duct epithelial cells in control liver specimens; **B:** LFA-1 immunoreactivity in portal lymphoid cells, negative in interlobular bile ducts and sparse expression in bile duct epithelial cells; **C:** Marked ICAM-1 immunoreactivity on the plasma membrane on the luminal side of bile ductules or possibly small blood vessels. Some lymphocytes around the bile ducts were also positive for ICAM-1. Arrowheads denote localization of ICAM-1 (arrows); **D:** LFA-1 immunoreactivity in lymphocytes around and among damaged bile ducts (arrowheads). Original magnification; ×400, hematoxylin counterstained.

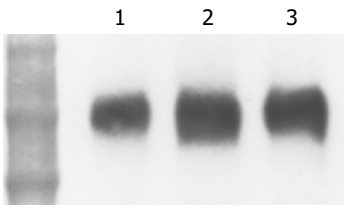

Figure 3 Western blot analysis of expression of ICAM-1 protein in human control and PBC liver tissue. Samples containing 20 μg protein were subjected to SDS/PAGE (4-20% gel) and analyzed by blotting. ICAM-1 was found in abundance in PBC liver tissues. Lanes 2 and 3: PBC liver tissue, lane 1: control liver tissue. Positions of molecular mass markers are shown (ku).

in 8 of the 10 cases. LFA-1 immunoreactivity was found in CoH in 4 of the 10 PBC cases and in bile ductules in 7 of the 10 cases. The extent of immunoreactivity (number of immunogold particles per unit CoH or bile ductule) was also stronger in bile ductules than in CoH. No immunogold–silver complex particles for ICAM-1 and LFA-1 were found in bile ductules and CoH of control liver tissues.

DISCUSSION

Bile duct inflammation and destruction are the fundamental lesions of PBC[25]. Interlobular bile ducts with external diameters of 30-100 μm are selectively affected, displaying variable necrotic and proliferative changes of biliary epithelial cells, as well as periductal lymphoplasmacytic infiltration. These findings are also frequently noted around damaged bile ducts, especially in the early histologic stages of the disease[25]. In our immunohistochemical study, ICAM-1 was strongly expressed on damaged bile ducts and infiltrating inflammatory cells, while LFA-1 was expressed on infiltrating lymphocytes. The presence of ICAM-1/LFA-1 linkage has been reported in CNSDC in PBC[16,17].

In our previous study, we correlated protein and mRNA expression of ICAM-1 and LFA-1 by conducting immunohistochemical and *in situ* hybridization studies on serial sections of CNSDC lesions[26]. We demonstrated abundant protein and mRNA expression of ICAM-1 on damaged biliary epithelial cells and LFA-1 on lymphocytes in CNSDC lesions, strongly suggesting the ICAM-1/LFA-1 linkage[26].

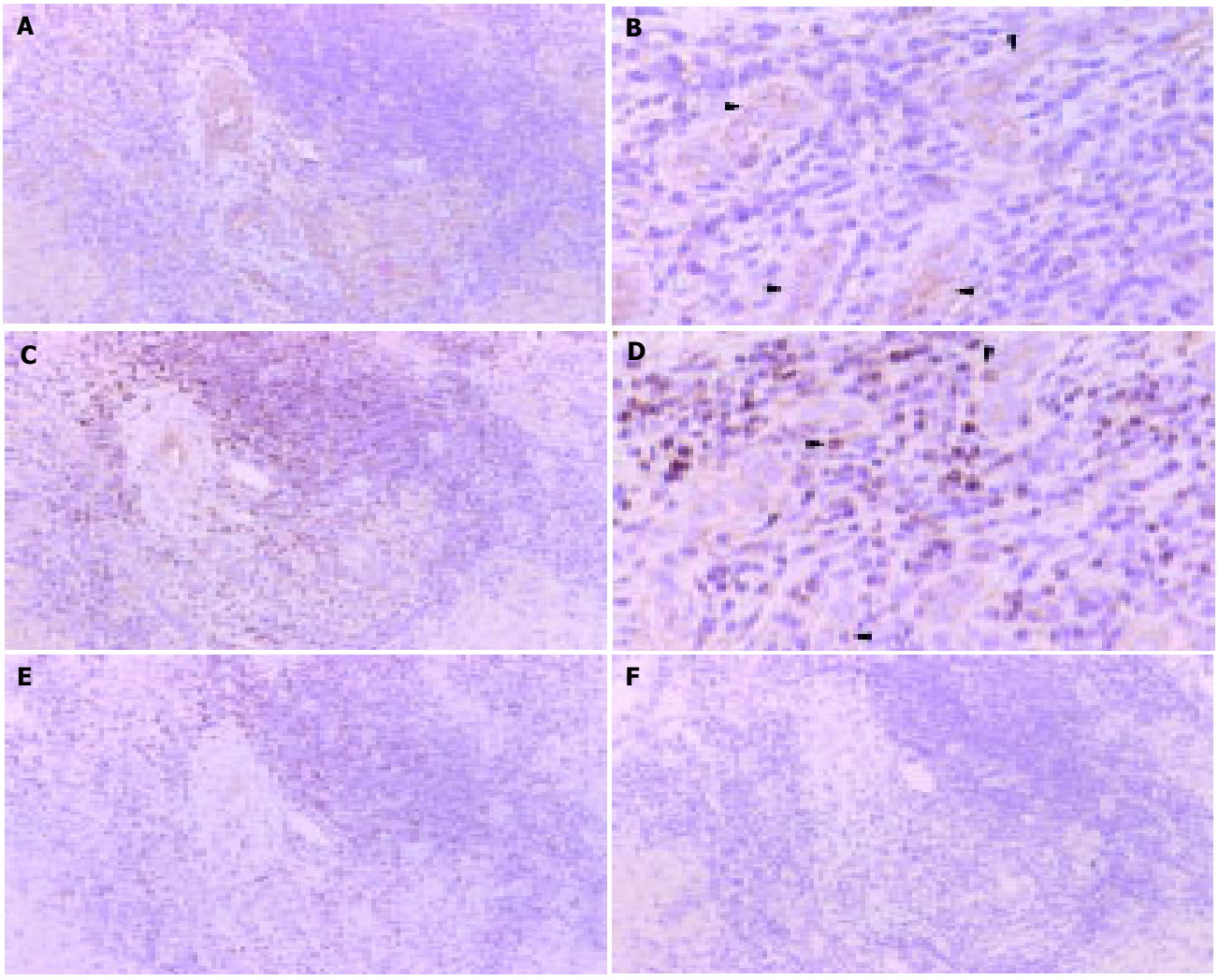

Figure 4 Localization of ICAM-1 (**A** and **B**) and LFA-1 (**C** and **D**) mRNA at bile ductules in PBC liver tissue by *in situ* hybridization with CSA. **A:** ICAM-1 mRNA was expressed in a cytoplasmic pattern on epithelial cells of bile ductile. (**A:** ×100 and **B:** ×300) Arrowhead denotes reaction product; **C:** LFA-1 mRNA is expressed in a cytoplasmic pattern in lymphocytes around bile ductile. (**C:** ×100 and **D:** ×300). Negative controls: **E:** ICAM-1 sense probe, **F:** LFA-1 sense probe. All panels: color was developed by DAB chromogen and hematoxylin counterstained. Arrowhead denotes reaction product.

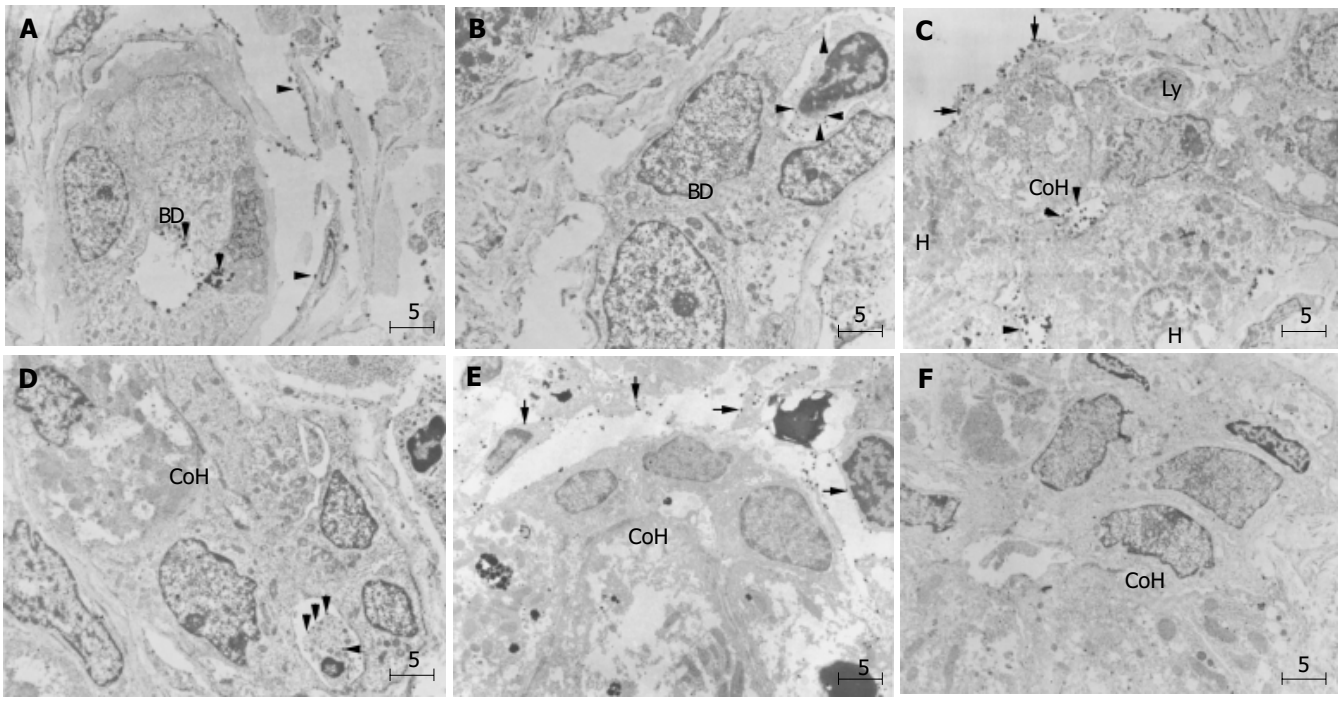

Figure 5 Immunoelectron microscopic findings of ICAM-1 (**A, C,** and **E**) and LFA-1 (**B, D,** and **F**) in periportal small bile ductule and canal of Hering in PBC liver. **A:** Gold-labeled ICAM-1 particles on the surface of cholangiocytes (arrowhead) facing the lumen of small bile ductule, a small portal or peripheral blood vessel, and also on sinusoidal endothelial cells (arrowheads). BD denotes bile ductule; **B:** Lymphocytes with dense labeling of LFA-1 (arrowhead) around small ductule; **C:** Gold-labeled ICAM-1 particles on the luminal surfaces of hepatocytes and cholangiocytes of CoH, on bile canaliculus and also on sinusoidal endothelial cells (arrows); **D:** Lymphocytes densely labeled with LFA-1 (arrows) on the basolateral membrane of cholangiocytes of the CoH; **E:** No ICAM-1 immunoreactivity show immature cells resembling progenitor cells (asterisk) in CoH, and these cells; **F:** No infiltration of lymphocytes is observed around the progenitor-like cells (asterisk). Bar, 5 μm; BD, bile ductile; Ly, lymphocyte; CoH, canal of Hering; H. hepatocyte. Uranyl acetate stain.

Frequent and variable infiltration of lymphocytes, mainly T cells, and other inflammatory cells of the biliary epithelium has been reported in PBC[27]. Some lymphocytes infiltrate by crossing the basement membrane of bile ducts. These changes appear as necro-inflammatory lesions inside the basement membrane of bile ducts and ductules.

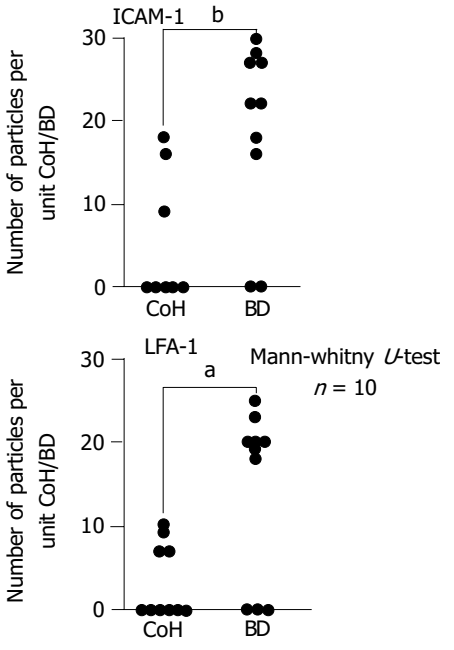

Figure 6 Semi-quantitative analysis of immunogold-silver complex particles on epithelial cells of bile ductules and cholangiocytes of CoH enumerated on immunoelectron micrographs (expressed in number of particles per unit CoH or small bile ductule). Immunoreactivity was significantly greater on bile ductules (Mann-Whitney test). BD, bile ductile; CoH, canal of Hering. [a]$P<0.05$, [b]$P<0.01$ *vs* CoH.

Our immunoelectron microscopic study has confirmed for the first time the ultrastructural localization of ICAM-1 on cholangiocytes and LFA-1 on infiltrating inflammatory cell in damaged CoH. The lymphocytes and other inflammatory cells then penetrated the peribiliary vascular plexus and portal venules, and migrated into perivenular tissue toward the bile ducts[12]. When early stage PBC specimens were immunostained for cytokeratin 19 and HLA-DR, the CoH were found mostly around portal tracts in stages 2 and 3 PBC, but they were destroyed in concert with the destruction of bile ductules[28]. Therefore, CoH in PBC specimens are difficult to be depicted by immunohistochemistry using light microscopy. Our immunoelectron microscopic study successfully demonstrated the ultrastructural localization of ICAM-1 and LFA-1 on CoH.

Previous studies of cell adhesion molecules, especially ICAM, in PBC have reported conflicting results. Adams *et al*.[14], reported a series of 13 patients with PBC studied at liver transplantation and found that ICAM was expressed on interlobular bile ducts and proliferating bile ductules. In contrast, Broome *et al*.[29], found ICAM in 3 of 10 patients with PBC while almost all patients expressed HLA-DR on biliary epithelium. Bloom *et al*.[30] found ICAM-1 expression on bile ducts in two of seven cases of early disease and in only one of five patients with stage three or four disease. According to these reports, ICAM-1 expression in PBC is not very common and not clearly associated with a particular

disorder. Using immunoelectron microscopy, we found that 8 of 10 PBC patients expressed ICAM-1 and 7 of 10 patients expressed IFA-1 on bile ductules. The higher rate probably reflects the higher sensitivity of our method.

In this study, we observed membranous staining of hepatocytes and bile ductules with different intensity with ICAM-1 antibodies (Figure 1C) in PBC. However, ICAM-1 expression on hepatocytes is indefinite or only faint in normal livers. These findings may suggest the involvement of immune-mediated hepatocytolysis related to expression and presentation of target antigens[12].

Bile duct loss can be evaluated semi-quantitatively by calculating the ratio of portal tracts devoid of interlobular bile ducts and also the proportion of hepatic arterial branches without parallel running interlobular bile ducts[12]. Regrowth of bile ducts has been reported, and a ductular reaction precedes the reappearance of neo-bile ducts. In this process, hepatic stem cells or progenitor cells migrate from the periportal area into the biliary tree[31]. On the other hand, in rat liver injury, the role of ICAM-1 is to adhere to neutrophils, and excessive parenchymal apoptosis may be a signal for this neutrophil-induced inflammatory and necrotic reaction[32]. Apoptosis of bile ductules could be one of the processes that explain the reduced proliferation of bile ductules[33]. Therefore, strong expression of ICAM-1 on bile ductules may be a cause of the reduction in proliferation of bile ductules[25,33].

Our semi-quantitative study of immunogold-silver complex in bile ductile epithelium and cholangiocytes in CoH of PBC liver revealed that the rate and intensity of ICAM-1 and IFA-1 expression were higher in the bile ductules than in the upstream CoH. The reason is that there are less mature cholangiocytes in the CoH. We observed cells with intermediate morphology in CoH, which may be progenitor cells labeled with ICAM-1 and LFA-1. Since the adhesion molecules appear to be expressed only on the mature cholangiocytes, this implies that the mature cholangiocytes are targeted for autoimmune destruction in PBC. Destruction in the CoH upstream of bile ductules also occurs because of the presence of mature cholangiocytes. Recently, a human bipotent liver progenitor cell line has been established, which shows comparable immunophenotype restricted to bile neoductules[34]. The mechanisms of how progenitor cells are protected from destruction by the host immune system should be studied.

REFERENCES

1 **Hering E.** Uber den bau der Wirbeltiereber, Sitzber. *Akad wiss Wien Math Naturic KL* 1865; **54**: 496-515
2 **Steiner JW,** Carruthers JS. Studies on the fine structure of the terminal branches of the biliary tree. *Am J Pathol* 1961; **38**; 639-661
3 **Watanabe N,** Tsukada N, Smith CR, Phillips MJ. Motility of bile canaliculi in the living animal- implications for bile flow. *J Cell Biol* 1991; **113**: 1069-10802
4 **Ishii K,** Phillips MJ. *In vivo* contractions of the duct of Hering. *Hepatology* 1995; **22** (4 Pt 2): 159
5 **Nonomura A,** Kono N, Mizukami Y, Nakanuma Y, Matsubara F. Histological changes in the liver in experimental graft-versus-host disease across minor histocompatibility barriers. IV. A light and electron microscopic study of the periportal changes. *Liver* 1991; **11**: 278-286
6 **Theise ND,** Saxena R, Portmann B, Thung SN, Yee H, Chiriboga L, Kumar A, Crawford JM. The canals of Hering and hepatic stem cells in humans. *Hepatology* 1999; **30**: 1425-1433
7 **Kaplan MM.** Primary biliary cirrhosis. *N Engl J Med* 1987; **316**: 512-528
8 **James SP,** Hoofnagle JH, Strober W. Primary biliary cirrhosis: a model autoimmune disease. *Ann Intern Med* 1983; **99**: 500-512
9 **Thomas HC,** Potter BJ, Sherlock S. Is primary biliary cirrhosis an immunocemplex disease? *Lancet* 1977; **2:** 1216-1263
10 **Wands JR,** Dienstag JL, Bhan AK, Feller ER, Isselbacher KJ. Circulating immune complexes and complement activation in primary biliary cirrhosis. *N Engl J Med* 1978; **298**: 233-237
11 **Cancellieri V,** Scaroni C, Vernace SJ, Schaffner F, Paronetto F. Subpopulation of T lymphocyte in primary biliary cirrhosis. *Clin Immunol Immunopathol* 1981; **20**: 255-260
12 **Nakanuma Y,** Yasoshimura M, Tsuneyama K, Harada K. Histopathology of primary biliary cirrhosis with emphasis on expression of adhesion molecules. *Semi Liver Dis* 1997; **17**: 35-47
13 **Volpes R,** Van Den Oord JJ, Desmet VJ. Immunohistochemical study of adhesion molecules in liver inflammation. *Hepatology* 1990; **12**: 59-65
14 **Adams DH,** Hubscher SG, Shaw J, Johnson GD, Babbs C, Rothlein R, Neuberger JM. Increased expression of ICAM-1 on bile ducts in primary biliary cirrhosis and primary sclerosing cholangitis. *Hepatology* 1991; **14**: 426-443
15 **Altmann DM,** Hogg N, Trowsdale J, Wilkinson D. Co-transfection of ICAM-1 and HLA-DR reconstitutes human antigen presenting cell function in mouse L lines. *Nature* 1990; **338**: 512-514
16 **Kaneko H,** Oda M, Yokomori H, Kazemoto S, Kamegaya Y, Komatsu H, Tsuchiya M. Immunohistochemical microscopic analysis of bile duct destruction in primary biliary cirrhosis: Involvement of intercellular adhesion molecules. *Int Hepatol Commun* 1994; **2**: 271-276
17 **Yasoshima M,** Nakanuma Y, Tsuneyama K, van de Water J, Gershwin ME. Immunohistochemical analysis of adhesion molecules in the micro-environment of portal tracts in relation to aberrant expression of PDC-E2 and HLA-DR on the bile ducts in primary biliary cirrhosis. *J Pathol* 1995; **175**: 319-325
18 **Ohta Y.** Diagnostic criteria for primary biliary cirrhosis. *Acta Hepatol Jpn* 1992; **33**: 657
19 **Mclean IW,** Nakane PK. Periodate-lysine-paraforaldehyde fixative: a new fixative for immunoelectron microscopy. *J Histochem Cytochem* 1974; **22**: 1077-1083
20 **Thisted M,** Just T, Pluzek KJ, Petersen KH, Hyldig-Nielsen JJ, Godtfredsen SE. Detection of immunoglobulin kappa light chain mRNA in paraffin sections by *in situ* hybridization using peptide nucleic acid probes. *Cell Vision* 1996; **3**: 358-363
21 **Simmons D,** Makgoba MW, Seed B. ICAM, an adhesion ligand of LFA-1, is homologous to the neural cell adhesion molecule NCAM. *Nature* 1988; **331**: 624-627
22 **Larson RS,** Corbi AL, Berman L, Springer T. Primary structure of the leukocyte function-associated molecule-1 alpha subunit: an integrin with an embedded domain defining a protein superfamily. *J Cell Biol* 1989; **108**: 703-712
23 **Kerstens HM,** Poddighe PJ, Hanselaar AG. A novel in situ hybridization signal amplification method based on the deposition of biotinylated tyramine. *J Histochem Cytochem* 1995; **43**: 347-352
24 **Fujimori O,** Nakamura M. Protein A gold-silver staining methods for light microscopic immunohistochemistry. *Arch Histol Jap* 1985; **48**: 449-452
25 **Nakanuma Y,** Ohta G. Quantitation of hepatic granulomas and epitheloid cells in primary biliary cirrhosis. *Hepatology* 1983; **3**: 423-427
26 **Yokomori H,** Oda M, Yoshimura K, Nomura M, Ogi M, Wakabayashi G, Kitajima M, Ishii H. Expression of intercel-

lular adhesion molecule-1 and lymphocyte function-associated antigen protein and messenger RNA in primary biliary cirrhosis. *Internal Med* 2003; **42**: 947-954

27 **Yamada G,** Hyodo I, Tobe K, Mizuno M, Nishihara T, Kobayashi T, Nagashima H. Ultrastructural immunocytochemical analysis of lymphocytes infiltrating bile duct epithelium in primary biliary cirrhosis. *Hepatology* 1986; **6**: 385-391

28 **Saxena R,** Hytiroglou P, Thung SN, Theise ND. Destruction of canals of Hering in primary biliary cirrhosis. *Hum Pathol* 2002; **33**: 983-988

29 **Broome U,** Hultcrantz R, Forsum U. Lack of concomitant expression of ICAM-1 and HLA-DR on bile duct cells from patients with primary sclerosing cholangitis and primary biliary cirrhosis. *Scand J Gastroentel* 1993; **28**: 126-130

30 **Bloom S,** Fleming K, Chapman R. Adhesion molecule expression in primary sclerosing cholangitis and primary biliary cirrhosis. *Gut* 1995; **36**: 604-609

31 **Gerber MA,** Thung SN. Liver stem cells and development. *Lab Invest* 1993; **68**: 261-263

32 **Kobayashi A,** Imamura H, Isobe M, Matsuyama Y, Sorda J, Matsunaga K, Kawasaki S. Mac-1(CD11b/CD18) and intercellular adhesion molecule-1 in ischemia-reperfusion injury of rat liver. *Am J Physiol* 2001; **281**: G577-585

33 **Bhathal PS,** Gall JA. Deletion of hyperplastic biliary epithelial cells by apoptosis following removal of the proliferative stimuli. *Liver* 1985; **5**: 311-325

34 **Parent R,** Marion MJ, Furio L, Trépo C, Petit MA. Origin and characterization of a human bipotent liver progenitor cell line. *Gastroenterology* 2004; **126**: 1147-1156

Science Editor Wang XL **Language Editor** Elsevier HK